



HHS Public Access

Author manuscript

J Hazard Mater. Author manuscript; available in PMC 2016 September 15.

Published in final edited form as:

J Hazard Mater. 2015 September 15; 295: 97–103. doi:10.1016/j.jhazmat.2015.03.069.

Potential Explosion Hazard of Carbonaceous Nanoparticles: Explosion Parameters of Selected Materials

Leonid A. Turkevich*,

Centers for Disease Control and Prevention, National Institute for Occupational Safety and Health, Division of Applied Research and Technology, 1090 Tusculum Avenue, MS-R7, Cincinnati, OH 45226 USA

Ashok G. Dastidar,

Fauske & Associates, LLC, 16W070 83rd Street, Burr Ridge, IL 60527 USA

Zachary Hachmeister, and

Fauske & Associates, LLC, 16W070 83rd Street, Burr Ridge, IL 60527 USA

Michael Lim

Fauske & Associates, LLC, 16W070 83rd Street, Burr Ridge, IL 60527 USA

Abstract

Following a previous explosion screening study, we have conducted concentration and ignition energy scans on several carbonaceous nanopowders: fullerene, SWCNT, carbon black, MWCNT, graphene, CNF, and graphite. We have measured minimum explosive concentration (MEC), minimum ignition energy (MIE), and minimum ignition temperature (MIT_{cloud}) for these materials. The nanocarbons exhibit $MEC \sim 10^1\text{--}10^2 \text{ g/m}^3$, comparable to the MEC for coals and for fine particle carbon blacks and graphites. The nanocarbons are confirmed mainly to be in the St-1 explosion class, with fullerene, at $K_{St} \sim 200 \text{ bar-m/s}$, borderline St-1/St-2. We estimate $MIE \sim 10^2 - 10^3 \text{ J}$, an order of magnitude higher than the MIE for coals but an order of magnitude lower than the MIE for fine particle graphites. While the explosion severity of the nanocarbons is comparable to that of the coals, their explosion susceptibility (ease of ignition) is significantly less (i.e. the nanocarbons have higher MIEs than do the coals); by contrast, the nanocarbons exhibit similar explosion severity to the graphites but enhanced explosion susceptibility (i.e. the nanocarbons have lower MIEs than do the graphites). $MIT_{cloud} > 550^\circ\text{C}$, comparable to that of the coals and carbon blacks.

Keywords

explosion hazard; dust; carbon; nanoparticle; nanomaterials

*corresponding author: LLT0@cdc.gov, Phone: (513) 841 4518, Fax: (513) 841 4545.

Disclaimers

The findings and conclusions in this report are those of the authors and do not necessarily represent the views of the National Institute for Occupational Safety and Health. Mention of product or company name does not constitute endorsement by the Centers for Disease Control and Prevention.

None of the authors has a financial relationship with a commercial entity that has an interest in the subject of this manuscript.

1. Introduction

This is the second of two articles describing our work on the explosibility of nanoscale carbonaceous materials. Our first article [1] surveyed the general potential for these materials to explode. This second article reports detailed explosion parameter measurements on selected materials from that initial screening survey.

In [1], we reported on an explosion survey of a variety of carbon nanomaterials: fullerene, single-walled carbon nanotubes (SWCNTs), multi-walled carbon nanotubes (MWCNTs), carbon nanofibers (CNFs), carbon blacks, graphites, graphene, and diamond. In that survey, we attempted to explode these powders at a fixed dust concentration ($c = 500 \text{ g/m}^3$) with an initiating energy of 5 kJ; explosion parameters at that concentration were reported as maximum explosion pressure, $P_m(500)$, and explosion severity index, $K(500) = V^{1/3}dP/dt|_{max}(500)$. From that survey, we concluded that each of these materials has the potential to explode, and with a severity that places it tentatively in the St-1 explosion class. In this paper, we report on a more detailed examination of the explosion parameters (P_{max} , K_{St} , MEC, MIE) for a representative set of these materials.

1.1 Previous Work

Dust explosion texts [2,3] do not discuss the explosion of powders of particles smaller than $10 \mu\text{m}$. The IFA explosion database [4] tabulates dust explosivity test data for micrometer-, but not nanometer-, sized powders. A literature review [5] of the explosion and flammability hazards of nanopowders primarily discusses micron-sized powders. The limited nanomaterial explosibility data motivated our earlier screening study [1] and the present, more detailed, investigation of explosion parameters.

There is an extensive literature on the explosion parameters for coal dust [1]. Typically, $P_{max} \sim 6 - 7 \text{ bar}$, and $K_{St} \sim 40 - 60 \text{ m-bar/s}$; the minimum explosive concentration can be as low as MEC $\sim 60 \text{ g/m}^3$; the minimum ignition energy may be as low as MIE $\sim 30 \text{ mJ}$; and the minimum cloud ignition temperature is in the range MIT $\sim 450 - 1100^\circ\text{C}$.

Explosion studies have also been conducted on several pure carbon systems: carbon blacks [6–8] and graphite [9,10]. These are also summarized in [1]: $P_{max} \sim 6 - 8 \text{ bar}$, $K_{St} \sim 10 - 140 \text{ m-bar/s}$, MEC $\sim 40 - 150 \text{ g/m}^3$, MIT $\sim 650 - 900^\circ\text{C}$, all comparable to the coals. The minimum ignition energy, MIE $\sim 10^0 - 10^1 \text{ kJ}$, was only measured for the fine particle graphites, and this is several orders of magnitude higher than the MIE for the coals. With the exception of the graphite MIE, the explosion parameters for finer carbon materials are generally quite similar to those of the coarser coals.

1.2 Recent Nanopowder Work

Using the standard 20-L explosion sphere [11,12], Vignes et al. [13] assessed the explosion severity (P_{max} , K_{St}) and explosion sensitivity (MIE, MEC) of various carbon black powders (Corax N115, Thermal Black N990, Corax N550, Printex XE2), one unidentified carbon nanotube (which we believe to be an Arkema MWCNT), and nano-Al. These Nanosafe2 results have been reported in several places [14–16], not always with identical values. Bouillard et al. [14,15,17] highlighted the high potential for explosion risks of only the

metallic nanoparticles in manufacturing facilities. For both the carbon blacks and the Nanosafe MWCNT [13], MEC $\sim 60 \text{ g/m}^3$ (comparable to the coals) and MIE $> 1 \text{ J}$ (an order of magnitude higher than that of the coals); MIT was not determined.

In a recent review [18], explosibility data on nanomaterials is taken mainly from the Nanosafe2 project.

1.3 Previous Results on the Size-Dependence of Explosion Parameters

1.3.1 Explosion severity—As particle size decreases (and specific surface area increases), the explosion severity increases [1].

1.3.2 Minimum explosive concentration (MEC)—The MEC, the lowest dust concentration at which an ignition can be achieved, typically decreases as the particle size decreases but then exhibits a plateau below a limiting particle size [3, 19]; however, Pittsburgh coal may exhibit a shallow minimum in MEC as a function of particle size at $d \sim 30 \mu\text{m}$ [20].

For low volatility (sub- $20 \mu\text{m}$) Pocahontas coal fines, MEC $\sim 80 \text{ g/m}^3$; for high volatility (sub- $20 \mu\text{m}$) Pittsburgh coal fines, MEC $\sim 85 \text{ g/m}^3$ [20]. For polyethylene, MEC exhibits a plateau at 50 g/m^3 for $d < 80 \mu\text{m}$ [3, 19], although perhaps MEC $\sim 30 \text{ g/m}^3$ for $d \sim 10 \mu\text{m}$ [21].

For the uncharacterized Nanosafe MWCNT [13], MEC $\sim 60 \text{ g/m}^3$, comparable to that found for various coals and carbon blacks [1, 15].

1.3.3 Minimum ignition energy (MIE)—The MIE, the minimum spark energy required to ignite a dust cloud, strongly depends on particle size, with no obvious plateau, even at micrometer particle sizes [3]. MIE should vary with the cube of the particle diameter [22]. Experimental results for polyethylene powder are consistent with this scaling [3, 23, 24]; for particle sizes in the range $25 - 250 \mu\text{m}$, $10 \text{ mJ} < \text{MIE} < 3000 \text{ mJ}$ (the low end of this range is only slightly higher than the MIE for gases and vapors [24]).

For metallic nanopowders, MIE $< 1 \text{ mJ}$ [23, 25, 26]. This low MIE puts these nanopowders at a higher ignition risk than similar micrometer-sized dusts, e.g. ignition as a result of electrostatic spark, collision or mechanical friction [18, 23, 25]. It is important to assess whether carbonaceous nanopowders exhibit such low MIE values.

1.3.4 Minimum Ignition Temperature (MIT)—The MIT, the lowest temperature at which a dust cloud or a dust layer will propagate combustion, appears to decrease with decreasing particle size [8] and may be concentration dependent [27].

Using isothermal thermogravimetry and thermal differential analysis, NanoSafe determined [14] onset temperatures for combustion, but not dust cloud or layer explosion temperatures.

As MIT has not been measured previously for any carbonaceous nanomaterials, our results represent the first such measurements and, as such, are an important quantification of nanocarbon explosion susceptibility.

1.4 Mechanisms that Yield a Limiting Particle Size

1.4.1 Limiting Particle Size arising from Reaction Mechanism—A limiting particle size can be understood in the context of the various steps in the reaction mechanism [1].

1.4.2 Limiting Particle Size arising from Agglomeration—It is suggested that agglomeration reduces the explosion severity of nanosized particles [18]. Agglomeration inhibits dispersion of fine, cohesive powders into a cloud of primary particles, since the aerodynamic forces are insufficient to disrupt the inter-particle attraction [14]. Similarly, agglomerates re-form in the dust cloud as a result of collision between particles, the coagulation rate being greater for the smaller particle sizes [23]. As a result of the incomplete dispersion and subsequent coagulation, the effective particle size will be greater than the primary (nm) particle size, thereby decreasing the explosion severity [28].

While the NanoSafe multi-walled carbon nanotubes have a very high specific surface area, when compared to carbon black (Corax, Printex, and Thermal Blacks), they exhibit 200 μm agglomerates; Bouillard et al. [14] argue that this large agglomerate size reduces the explosion severity of the carbon nanotubes, compared with that of the carbon blacks.

2. Experimental Methods

Explosion experiments were conducted at Fauske & Associates, LLC (Burr Ridge, IL).

2.1 Explosion Severity

Descriptions of the test method [11], protocol and correction factors have been discussed in [1]. The initial screening test [1] was performed at a nominal dust concentration $c = 500 \text{ g/m}^3$, and the explosion parameters were reported as $P_m(500)$, $K(500)$.

The Siwek 20-L chamber, used in our studies, is described in [1]. A slightly different 20-L chamber (USBM 20-L, also known as PRL 20-L) has been utilized at the US Bureau of Mines, Pittsburgh Research Lab [29–31] in their extensive studies of explosion hazards of coal dusts.

Dust dispersion is comparable in the USBM 20-L and 1- m^3 chambers [32]. Enhanced aggregate break-up occurs in the dispersion of coal dusts in the Siwek 20-L [33]; of the two Siwek designs, the rebound nozzle appears to be more aggressive in breaking up aggregates than the perforated annular nozzle. All three chambers yield uniform dust dispersions [33].

In the USBM 20-L apparatus, compressed air enters the chamber through a solenoid valve and then passes through the dust, dispersing it through a nozzle; the dust does not pass through the solenoid valve. In the earlier 1- m^3 chamber, the dispersion nozzle is a perforated semicircular spray pipe, similar in design to the perforated annular nozzle of the Siwek 20-L (although the current Fike design uses a rebound nozzle). In the 1- m^3 chamber, the dust agglomeration is not expected to be significantly affected as it passes through the pneumatic ball dispersion valve [32]. However, the different design of the outlet valve of the Siwek 20-L may induce agglomerate break-up [33].

Our results (Section 3) indicate that the explosion characteristics of the carbonaceous nanoparticle dusts do not depend on aggregate size. Since we have exclusively used the Siwek 20-L chamber, all of our different materials are dispersed and exploded under identical aggressive conditions, probably sufficient to break up any aggregates.

2.2 Concentration Scan to determine P_{max} , K_{St} and MEC

For the selected materials of this study, explosion testing was performed at several dust concentrations. For each concentration, c , we determine $P_m(c)$ and $K(c)$; the largest such values are reported as P_{max} and K_{St} . This also allows a determination of the MEC, the minimum concentration that the dust/air mixture will sustain a deflagration. As before, this testing was conducted in the spherical 20-L Siwek chamber, using a single 5 kJ ignition source [34]. Cashdollar and Chathrathi [32] compare the use of 20-L and 1-m³ chambers to obtain MEC.

2.3 Minimum Ignition Energy (MIE)

For the same selected materials, explosion testing was performed in the 20-L chamber with reduced ignition strengths, in order to determine the MIE of a dust cloud. The powder samples are dispersed in the apparatus, as before, and attempts are made to ignite the resultant dust cloud with pyrotechnic igniters of a known energy (0.25 kJ, 0.5 kJ, 1 kJ, 2.5 kJ).

Note that this measurement differs from ASTM E2019 [35], conducted in a MIKE-3 apparatus (manufactured by Kuehner AG, Basel, Switz.). The minimum igniter energy generated in the MIKE-3 apparatus is 1 mJ; for materials with a lower MIE (e.g. some of the nanometals), other measurement techniques must be used [36]. The materials tested here all exhibit higher MIEs than are typically measured with the MIKE-3 (whose maximum igniter energy is 1J), and this 'hard to ignite' feature motivated our alternative MIE protocol. Cashdollar [27] also discusses the difference between the stored electrical energy in a capacitive discharge and that actually delivered to a dust to electrically ignite an explosion.

2.4 Minimum Ignition Temperature (MIT) of a Dust Cloud Tests

The MIT_{cloud} , the minimum temperature at which a dust cloud will ignite when exposed to air heated in a furnace at local atmospheric pressure, is determined [37] using a BAM oven, manufactured by Kuehner AG, Basel, Switz.

An initial estimate of the MIT is made by heating the oven to $T = 600^{\circ}\text{C}$ and then switching off the power and allowing the temperature to fall. At intervals of $T = 50^{\circ}\text{C}$, a premeasured volume ($V = 1 \text{ mL}$) of dust is dispersed into the furnace with a blast of air. Ignition of the dust is identified as the observation (within 5 seconds of dispersion) of a flame exiting the flap at the rear of the oven.

MIT is then determined by a series of tests, conducted at stabilized temperatures near the estimate. The starting temperature is the lowest temperature for which flame was observed in the estimate test. These tests are conducted by decreasing the test temperature in $T = 10^{\circ}\text{C}$ increments until flame is no longer observed. For each test, a premeasured volume (V

= 1 mL) of dust is placed in the dust sample tube, which is then inserted into the furnace, and the dust is dispersed with a blast of air. At the highest temperature for which no flame is observed, two additional dust volumes ($V = 0.5\text{ mL}$, 2 mL) are tested. MIT is the lowest temperature at which a flame is observed at any of the tested concentrations.

The test equipment is calibrated by measuring the $\text{MIT}_{\text{cloud}}$ for *Lycopodium* (literature $\text{MIT}_{\text{cloud}} = 430^\circ\text{C}$).

2.5 Particle Sizing

Aggregate particle size was determined using a CILAS 1064 laser particle size analyzer (Compagnie Industrielle des Lasers, CILAS, Orleans, France), operated in the dry mode, where the powder is dispersed with compressed air. Diffraction from two laser beams ($\lambda_1 = 635\text{ nm}$, $\lambda_2 = 830\text{ nm}$) is fit [38] to Fraunhofer diffraction from a distribution of spherical particle sizes (the Fraunhofer model does not require a complex refractive index of the material as an input). Similar particle size distributions result from fitting the CILAS 1064 diffraction signal to Mie diffraction, where we have used the complex refractive index $n_r \sim 2$, $n_i \sim 1$ (appropriate for carbon black) for each of these carbonaceous materials; as expected, deviations between Mie and Fraunhofer fits are only apparent for $d < 1\ \mu\text{m}$. For all the materials studied, there is minimal sub-micron weight in the distributions; hence, we have only reported the Fraunhofer-derived particle size distributions.

2.6 Materials

Description of the materials is contained in [1]. Unless otherwise specified, materials parameters are those provided by the manufacturer. Of those materials, the following were selected for the current study: C60 fullerenes (Bucky USA, BU-602), SWCNT (SWeNT SG65), carbon black (Cabot Corp. Monarch 900), MWCNT (CheapTubes 030503), graphene (Angstrom N008-100-N), CNF (Pyrograf PR-19-XT-PS), graphite (AlfaAesar, natural microcrystalline).

3. Results

3.1 Explosion severity at $c = 500\text{ g/m}^3$ in Siwek chamber

Susceptibility of these carbonaceous materials to potential dust explosion hazard was previously evaluated in a series of systematic screening experiments [1]. This screening was conducted at nominal dust concentration $c = 500\text{ g/m}^3$, which represents fuel-rich (i.e. oxygen-limited) combustion. For each test sample, replicate explosions were conducted, with very reproducible results. Reported in [1] are $P_m(500)$ and $K(500) = V^{1/3} dP/dt|_{\text{max}}(500)$. Similar allotropes of carbon exhibit similar explosion characteristics [1].

3.2 Explosion severity (P_{max} , K_{St}) and MEC

For the seven selected materials of this study, we conducted more extensive testing, where we varied the mass of powder loaded in the Siwek chamber (concentration scan), retaining, however, the same ignition energy, 5 kJ , used in the screening study. For each concentration, we measured $P_m(c)$ and $dP/dt|_{\text{max}}(c)$. As the initial screening was conducted under fuel-rich conditions ($c = 500\text{ g/m}^3$), the screening explosions were not optimized; in all cases, higher

values of $P_m(c)$ and $dP/dt|_{max}(c)$ were obtained for concentrations $c < 500 \text{ g/m}^3$. The maximum values of these parameters that are obtained at the lower concentrations are reported in Table 1 as P_{max} (column 2), and K_{St} (column 4); the corresponding screening values (obtained at the higher $c = 500 \text{ g/m}^3$) are reported in Table 1 as $P_m(500)$ (column 3) and $K(500)$ (column 5). The minimum explosive concentration, the lowest concentration, at which an explosion may be sustained, is reported in Table 1 as the MEC (column 6). The characteristic velocity of the explosion front, constructed as $v \sim K_{St}/P_{max}$, is also reported in Table 1 (column 9).

3.3 Minimum ignition energy

We also conducted a scan of the ignition energy. In these experiments, the 5 kJ Sobbe pyrotechnic igniter was replaced with a succession of lower energy pyrotechnic igniters (0.25 kJ to 2.5 kJ). In all cases, significant reduction in the ignitor strength still initiated an explosion. Our best estimate of the minimum ignition energy, the lowest ignition energy which can initiate an explosion, is reported in Table 1 as the MIE (column 7).

3.4 Minimum Ignition Temperature MIT_{cloud}

Minimum ignition temperature results are reported in Table 1 (column 8) for fullerene and SWCNT; the remaining materials failed to auto-ignite at the highest temperature tested, $T = 600^\circ\text{C}$.

3.4 Particle Size

Primary particle size was quantified (from BET N_2 adsorption) by specific surface area, A , for all of the screened materials [1]. No correlation was found [1] between primary particle size and the explosion characteristics at $c = 500 \text{ g/m}^3$.

Aggregate particle size distributions were measured by light scattering (using the CILAS 1064 [38]) only for those seven materials that were more extensively studied. All seven of these materials exhibit (Figure 1) broad multimodal distributions in aggregate particle size. For each of these distributions, we have identified (see Supplemental Material) several parameters that characterize the distribution: the sizes, d_{mean} , and d_{50} , of the mean and mode of the distribution, the size, d_{dom} , of the dominant mode of the distribution, and the sizes, d_{max} and d_{min} , of the maximum and minimum identifiable modes. Since most of the weight of the distributions occurs at the larger aggregate sizes, the first four of these parameters (excluding d_{min}) are essentially equivalent characterizations.

4. Discussion

4.1 Overall Magnitudes of Explosion Parameters

As discussed in [1], these materials are all very similar in their explosion behavior. Maximum explosion pressures are in the range $4.0 \text{ bar} < P_m(500) < 6.8 \text{ bar}$, comparable to the coals and to the carbon blacks. The explosion severity index of these nanocarbons are in the wider range $4 \text{ bar-m/sec} < K(500) < 180 \text{ bar-m/sec}$, again comparable to the coals and to the carbon blacks. Thus, from the screening study [1], all of these nanocarbon materials seem to fall in the St-1 band.

As the fuel concentration is reduced, more optimal explosion conditions are achieved (Table 1) with slightly higher P_{max} and K_{St} (Figure 2). The most explosive material is fullerene ($P_{max} = 8.0$ bar); the least explosive material is graphite ($P_{max} = 6.3$ bar). These P_{max} values are comparable with those previously measured results for coals [39], carbon blacks [8] and graphite [10]. The material with the most rapid explosion kinetics is fullerene ($K_{St} = 199$ bar-m/sec); the material with the slowest explosion kinetics is the graphite ($K_{St} = 64$ bar-m/sec). These K_{St} values are comparable with those previously measured results for carbon blacks [8] and slightly higher than those measured for the coals [39] and graphite [10]. Consistent with the screening study [1], the explosion severity index, K_{St} , is highly correlated ($R^2 = 0.89$) with the maximum explosion pressure, P_{max} (Supplemental Material).

The characteristic velocities of the explosion fronts, $v = K_{St}/P_{max}$, are in the range $10 \text{ m/s} < v < 25 \text{ m/s}$, with, again, the fullerene having the most rapidly developing explosion and graphite and graphene the slowest developing explosion. Again, these are comparable [1] to the characteristic explosion velocities for the coals: $v \sim 6, 8 \text{ m/s}$ (Pocahontas, Pittsburgh standard) [20], $v \sim 22 \text{ m/s}$ (Marwell brown Victoria) [40].

The minimum explosive concentrations (Table 1) fall in the range $17 \text{ g/m}^3 < \text{MEC} < 92 \text{ g/m}^3$, with fullerene at the low end and graphite at the high end. With the exception of the low fullerene, these MECs are comparable to the MECs for the coals [20] and for the carbon blacks [6–8, 41, 42] and for graphite [10]. The MEC is highly correlated ($R^2 = 0.74$) with P_{max} and ($R^2 = 0.80$) with K_{St} (Supplemental Material).

The minimum ignition energies, $0.25 \text{ kJ} < \text{MIE} < 2.5 \text{ kJ}$, are significantly higher (Table 1) than those for the coals [1]: $30 \text{ mJ} < \text{MIE} < 70 \text{ mJ}$ [43], $\text{MIE} \sim 190 \text{ mJ}$ [40], $30 \text{ mJ} < \text{MIE} < 60 \text{ mJ}$ [39], $\text{MIE} \sim 60 \text{ mJ}$ [20]. Previous measurements [17] on the carbon blacks indicate $\text{MIE} > 1 \text{ J}$; however, the nanocarbon MIE are slightly lower than those of the previously measured graphites, $1 \text{ kJ} < \text{MIE} < 10 \text{ kJ}$ [10]. The MIE is poorly correlated ($R^2 = 0.24$) with P_{max} and ($R^2 = 0.30$) with K_{St} ; there is a similar lack of correlation ($R^2 = 0.22$) between MIE and MEC (Supplemental Material).

The cloud minimum ignition temperatures for fullerene and SWCNT are lower ($550^\circ\text{C} < \text{MIT}_{cloud} < 570^\circ\text{C}$) than the MIT_{cloud} for the carbon blacks [8] but comparable to the MIT_{cloud} for the coals [39]; the remaining nanocarbons have $\text{MIT}_{cloud} > 600^\circ\text{C}$, which is comparable to the carbon blacks [8] but slightly higher than the coals [39].

Thus the explosion severity for the nanocarbons is comparable to that of both the coals and the graphites. As measured by MEC, the explosive susceptibility of the nanocarbons is comparable to that of both the coals and the graphites. As measured by MIE, the nanocarbons are less explosively susceptible than the coals (higher MIE) but more explosively susceptible than the graphites (lower MIE). The MIT measurements do not permit a similar definitive comparison.

4.2 Particle Size Effects—Primary Particle Size

We have measured BET specific surface area, as an indicator of primary particle size [1]. There appears to be no correlation between the strength of the explosion, $P_m(500)$, and the

particle size (specific surface area); the energy released in the oxidation of the carbon is very similar for all the different forms of carbon, i.e. $P_m(500)$ lies in a narrow band, irrespective of BET specific surface area. Similarly, the kinetics of the explosion, as measured by $K(500)$, is uncorrelated with particle size; i.e. $K(500)$ vs. BET specific surface area is a scatter plot.

4.3 Particle Size Effects—Aggregate Size

We believe that aggregation of the primary particles also is not a significant determinant of the explosion parameters. Firstly, there is no evidence of any tightly bound aggregates from our electron micrographs, either before or after explosion [1]. Secondly, the clustering of materials by allotrope (Figure 5 of [1]) would require aggregation to be correlated with allotrope—there is no indication of such behavior. Thirdly, arguments [15] in favor of aggregation influencing the explosion parameters are based on a qualitative evaluation of the aggregation state of the nanomaterials and completely neglect the differences in allotrope of the materials being compared. Again, we believe that aggregation has a minimal effect on the explosion parameters of the carbonaceous nanomaterials.

We have measured (Figure 1) aggregate particle size distributions with light scattering (CILAS 1064). We have attempted to correlate the various parameters that characterize those distributions with the measured explosion parameters. The scatter plots, with their respective, weak, correlation coefficients, are reported in the Supplemental Material. The several parameters, d_{mean} , d_{50} , d_{dom} , d_{max} are essentially equivalent, with weak correlations ($R^2 \sim 0.6$) to P_{max} and ($R^2 \sim 0.6$) to K_{St} ; d_{min} is also poorly correlated to P_{max} ($R^2 \sim 0.1$) and to K_{St} ($R^2 \sim 0.2$).

Problematic for the NanoSafe hypothesis [15] is that we find, statistically, that the smaller the aggregate, the less explosive the material, whereas the NanoSafe hypothesis has the smaller aggregates to be more explosive. Similarly (see Supplemental Material), the MEC exhibits a weak negative statistical correlation with aggregate size, which is again counterintuitive in that, statistically, the smaller aggregates would appear to require a higher fuel threshold.

We conclude that aggregate particle size has little influence on the severity of, or on the threshold for, the carbonaceous explosions.

The above argument is not strictly correct. Materials of the same allotrope, but with different aggregate particle size, should be compared; such data is not yet available. From our limited data set, we may only conclude that the variation of explosion parameters with aggregate size is less important than the variation that we have already observed between the different allotropes.

4.4 Explosion Mechanism

We believe that the electron micrographs of the exploded material [1] are revelatory of a common explosion pathway for these materials. Carbon atoms are ‘boiled off’ of the solid particles, and the oxidation reaction takes place in the gas phase. At high temperatures, $2\text{C} + \text{O}_2 \rightarrow 2\text{CO}$. Following the reaction, as the system cools, the CO disproportionates [43], 2

$\text{CO} \rightarrow \text{C (soot)} + \text{CO}_2$ (Boudouard reaction). The reaction mechanism is universal; hence the ubiquity of the soot balls observed [1] in the electron micrographs of the exploded material.

The structure of the solid carbon fuel has two effects. The different allotropes of carbon have slightly different heats of fusion, resulting in slight differences in the thermodynamics of the explosion; thus all the materials have comparable values of P_{max} , but there is a tendency for the materials to be clustered in P_{max} by allotrope [1]. Similarly, differences in the activation energy to ‘boil’ the carbon atoms off of the solid particles will result in slight differences in kinetics; again, there is a tendency for the materials to be clustered in K_{St} by allotrope [1].

4.5 Thermodynamics

It is instructive to estimate P_{max} from the equilibrium thermodynamics of the reaction. At stoichiometry ($c \sim 200 \text{ g/m}^3$), all of the O_2 in the chamber reacts with just enough C to yield CO ($N_C = 2N_{\text{O}_2} = N_{\text{CO}}$), liberating the heat $H = h N_{\text{CO}} = 2 h N_{\text{O}_2}$, (where h is the enthalpy of reaction per mole of product, and where $N_{\text{CO}}, N_C, N_{\text{O}_2}$ are respectively the numbers of moles of CO produced and moles of C and O_2 consumed). H heats up the gas, with a temperature rise, $T = H/C_V$, where the heat capacity is just that of the gas $C_V = c_{air} (N_{air} - N_{\text{O}_2} + N_{\text{CO}}) = c_{air} (N_{air} + N_{\text{O}_2})$ (where c_{air} is the heat capacity per mole of air, and N_{air} is the number of moles of air in the chamber). The overpressure is given by

$$P_{max}/P_i = (N_{\text{O}_2}/N_{air}) * [1 + 2\Delta h/c_{air}T_i],$$

where T_i is the initial (absolute) temperature, and P_i is the initial (i.e. atmospheric) pressure. For air, $N_{\text{O}_2}/N_{air} = 0.20947$, and $c_{air} = 30.76 \text{ J/mol}^\circ\text{K}$; for the explosion of graphite, $h = 110.5 \text{ kJ/mol}$.

Below stoichiometry (i.e. $2[\text{C}] < [\text{O}_2]$), the amount of carbon $N_C = N_{\text{CO}} = 2a N_{\text{O}_2}$ is insufficient ($a < 1$) to react with all the O_2 . The heat released is reduced, $H = 2a h N_{\text{O}_2}$, as is the heat capacity of the gas, $C_V = c_{air} * (N_{air} + aN_{\text{O}_2})$, whence the overpressure is proportionately reduced,

$$P_m/P_i = \alpha * (N_{\text{O}_2}/N_{air}) * [1 + 2\Delta h/c_{air}T_i].$$

Above stoichiometry (i.e. $2[\text{C}] > [\text{O}_2]$), there is excess carbon available, $N_C = aN_{\text{CO}} = 2a N_{\text{O}_2}$ (with $a > 1$). While the heat released is the same as at stoichiometry, the heat capacity is augmented by that of the unreacted carbon, $C_V = c_{air} (N_{air} + N_{\text{O}_2}) + c_{carbon} 2(a-1) N_{\text{O}_2}$. The overpressure is correspondingly reduced by the heating of this unreacted carbon,

$$P_m/P_i = (N_{\text{O}_2}/N_{air}) * \{1 + 2\Delta h/c_{air}T_i * [1 + 2(\alpha - 1) * (c_{carbon}/c_{air}) * N_{\text{O}_2}/(N_{air} + N_{\text{O}_2})]^{-1}\}$$

P_{max} thus occurs at stoichiometry.

Using $c_{carbon} = 20.76 \text{ J/mol } ^\circ\text{K}$, appropriate for graphite, we may estimate $P_m(c)$, and this has also been included in Fig. 2. Despite the explosion being dynamic, equilibrium thermodynamics provides a good estimate of $P_m(c)$ and hence of P_{max} . Prior to the explosion front contacting the outer wall, the heat released from the explosion is thermally isolated, and the explosion chamber functions as a bomb calorimeter.

5. Conclusion

There is a concern that engineered carbon nanoparticles, when manufactured on an industrial scale, may present an explosion hazard. In our earlier study [1], explosion testing was performed on 20 different carbonaceous nanomaterials. These include several different codes of SWCNTs (single-walled carbon nanotubes), MWCNTs (multi-walled carbon nanotubes) and CNFs (carbon nanofibers), graphene, diamond, fullerene, as well as several different control carbon blacks and graphites. Explosion screening was performed in a 20-L explosion chamber, at a (dilute) concentration of 500 g/m^3 , using a 5 kJ ignition source. Samples typically exhibited overpressures of 5–7 bar, and deflagration index $K(500) = V^{1/3} (dP/dt)_{max} \sim 10 - 80 \text{ bar-m/s}$, which suggests that these materials are in European Dust Explosion Class St-1 (similar to cotton and wood dust). There was minimal variation between these different materials. The explosive characteristics of these carbonaceous powders are uncorrelated with primary particle size (BET specific surface area).

For the selected materials of this study (fullerene, SWCNT, carbon black, MWCNT, graphene, CNF, graphite), we have performed additional explosions i) at reduced concentrations (to identify P_{max} , K_{St} and minimum explosive concentration, MEC), and ii) at reduced ignition sources (to identify minimum ignition energy, MIE). We have also contacted the dusts with hot air to determine the minimum ignition temperature, MIT_{cloud} . These materials exhibit MEC $\sim 10^1 - 10^2 \text{ g/m}^3$, comparable to the MEC for coals, fine particle carbon blacks and graphites. The concentration scans also confirm that the earlier screening was performed under fuel-rich conditions (i.e. the maximum over-pressure and deflagration index exceed the screening values); e.g. the true fullerene $K_{St} \sim 200 \text{ bar-m/s}$, placing it borderline St-1/St-2, while the other materials remain in St-1. The materials exhibit minimum ignition energy in the range $0.25 \text{ kJ} < \text{MIE} < 2.5 \text{ kJ}$, significantly higher than the MIE for the coals and slightly lower than the MIE for the fine particle graphites. The materials exhibit minimum ignition temperatures $MIT_{cloud} > 550^\circ\text{C}$, comparable to the coals and carbon blacks.

We have argued for a universal mechanism of combustion of these different allotropes: carbon atoms are ‘boiled off’ of the solid particulates, and high temperature oxidation, $2\text{C} + \text{O}_2 \rightarrow 2\text{CO}$, occurs in the gas phase; as the system cools, the CO disproportionates $2\text{CO} \rightarrow \text{C} (\text{soot}) + \text{CO}_2$, generating the ubiquitous soot balls observed in the electron micrographs of the exploded material. Thermodynamics yields a good approximation of the overpressure at various solids concentrations. We also argued against a significant effect of either primary particle size or primary particle aggregation on the explosion parameters.

Supplementary Material

Refer to Web version on PubMed Central for supplementary material.

Acknowledgments

We thank the late Ken Cashdollar and Chi-Keung Man (both of NIOSH) for introducing us to the parameters and measurements necessary to characterize dust explosions. We thank Kevin Ashley, Eileen Birch, Scott Earnest, Doug Evans, Alberto Garcia (all of NIOSH) for careful reading of the manuscript.

This work was supported through the NIOSH Nanotechnology Research Center. We especially thank Paul Schulte (NIOSH) for the prescient recognition of the potential explosion hazard posed by these materials and for the encouragement of this research.

References

1. Turkevich LA, Fernback JE, Dastidar AG, Hachmeister Z, Lim M. Potential explosion hazard of carbonaceous nanoparticles. Survey of allotropes. 2014 unpublished.
2. Bartknecht, W. Dust Explosions—Course, Prevention, Protection. Springer-Verlag; Berlin: 1989.
3. Eckhoff, RK. Dust Explosions in the Process Industries. 3. Gulf Professional Publishing, Elsevier; Burlington, MA: 2003.
4. GESTIS-DUST-EX: <http://staubex.ifa.dguv.de/explosuche.aspx>, compiled by IFA (Institut fuer Arbeitsschutz der Deutschen Gesetzlichen Unfallversicherung).
5. Pritchard, DK. Literature Review—Explosion Hazards Associated with Nanopowders. Health and Safety Laboratory; Buxton, UK: 2004. HSL/2004/12
6. Seweryniak, M.; Maslon, J. Konferencja “Sadze Techniczne” (Jaszowiec, Poland Wyd) NIT i NM Pwr., No. 288, Konferencje. 1985. p. 177-190.cited in [8]
7. Seweryniak, M.; Kordylewski, W.; Maslon, J.; Wysocki, L. Wlasnosci Wybuchowe Sadz, Nauka i Technika Pozarnicza. 1989. p. 56-63.cited in [8]
8. Kordylewski W, Seweryniak M. Explosion and flammability properties of furnace carbon blacks. Archivum Combustionis. 1992; 12(1–4):153–160.
9. Denkevits, A.; Dorofeev, S. Report FZKA-6872 Forschungszentrum Karlsruhe GmbH (Karlsruhe). Technik und Umwelt. Inst. fuer Kern- und Energie-technik/Programm Kernfusion; 2003. Dust Explosion Experiments: Measurement of Explosion Indices of Graphite Dusts.
10. Denkevits A, Dorofeev S. Explosibility of fine graphite and tungsten dusts and their mixtures. J Loss Prev Process Ind. 2006; 19:174–180.
11. ASTM E1226. Standard test method for pressure and rate of pressure rise for combustible dust. ASTM International; West Conshohocken, PA: 2012.
12. NFPA 68. Standard on Explosion Protection by Deflagration Venting. National Fire Protection Association; Quincy, MA: 2007.
13. Vignes, A.; Traore, M.; Dufaud, O.; Perrin, L.; Bouillard, J.; Thomas, D. Assessing explosion severity of nanopowders with the 20 L sphere. 8th World Congress of Chemical Engineers; Montreal, Quebec, CAN. 23–27 Aug. 2009; paper 01350
14. Bouillard J, Vignes A, Dufaud O, Perrin L, Thomas D. Explosion risks from nanomaterials. Nanosafe 2008: Intl. Conf. on Safe Production and Use of Nanomaterials. J Phys Conf Series. 2009; 170:012032.
15. Bouillard J, Vignes A, Dufaud O, Perrin L, Thomas D. Ignition and explosion risks of nanopowders. J Hazardous Materials. 2010; 181:873–880.
16. Schuster, F.; Bouillard, J. NANOSAFE2: Safe production and use of nanomaterials European project No. 515843-2. 2005–2009. www.nanosafe2.org
17. Bouillard, J.; Vignes, A.; Dufaud, O.; Perrin, L.; Thomas, D. Safety aspects of reactive nanopowders. AIChE Annual Meeting; 8–13 Nov. 2009; Nashville, TN.

18. Worsfold SM, Amyotte PR, Khan FI, Dastidar AG, Eckhoff RK. Review of explosibility of nontraditional dusts. *Ind Eng Chem Res.* 2012; 51(2):7651–7655. republished as ‘Explosibility of non-traditional dusts’. *Hazardex* (July 2013): 16–23.
19. Hertzberg, M.; Cashdollar, KL. *Industrial Dust Explosions STP 958*. American Society for Testing and Materials; Philadelphia, PA: 1987. Introduction to dust explosions; p. 5-32.
20. Cashdollar KL. Coal dust explosibility. *J Loss Prev Process Ind.* 1996; 9:65–76.
21. Zalosh, R. Explosion Protection (chapter 3–15). In: DiNenno, P.J.; Drysdale, D.; Beyler, C.L.; Walton, W.D., editors. *SFPE Handbook of Fire Protection Engineering*. 4. National Fire Protection Association; Quincy, MA: 2008.
22. Kalkert N, Schecker H-G. Theoretische Ueberlegungen zum Einfluss der Teichengroesse auf die Mindestzuendenergie von Staebun. *Chemie Ingenieur Technik.* 1979; 51:1248–1249.
23. Eckhoff RK. Are enhanced dust explosion hazards to be foreseen in production, processing and handling of powders consisting of nm-particles? *Nanosafe 2010: Intl. Conf. on Safe Production and Use of Nanomaterials. J Phys Conf Ser.* 2011; 304:1–20.
24. Dobashi R. Risk of dust explosions of combustible nanomaterials. *Nanosafe 2008: Intl. Conf. on Safe Production and Use of Nanomaterials. J Phys Conf Series.* 2009; 170:012029.
25. Wu HC, Chang RC, Hsiao HC. Research of minimum ignition energy for nano titanium powder and nano iron powder. *J Loss Prev Process Ind.* 2009; 22:21–24.
26. Wu H, Kuo Y, Wang Y, Wu C, Hsiao H. Study on safe air transporting velocity of nanograde aluminum, iron, and titanium. *J Loss Prev Process Ind.* 2010; 23:308–311.
27. Cashdollar KL. Overview of dust explosibility characteristics. *J Loss Prev Process Ind.* 2000; 13:183–199.
28. Boilard, S. thesis. Dalhousie Univ; Halifax, Nova Scotia, CAN: Feb. 2013 *Explosibility of Micron- and Nano-Size Titanium Powders.*
29. Cashdollar KL, Hertzberg M. 20-L explosibility test chamber for dusts and gases. *Rev Sci Instr.* 1985; 56:596–602.
30. Cashdollar KL. Flammability of metals and other elemental dusts. *Process Safety Progress.* 1994; 13:139–145.
31. Cashdollar KL, Zlochower M. Explosion temperatures and pressures of metals and other elemental dust clouds. *J Loss Prev Process Ind.* 2007; 20:337–348.
32. Cashdollar KL, Chatrathi K. Minimum explosible dust concentrations measured in 20-L and 1-m³ chambers. *Combustion Sci Tech.* 1993; 87:157–171.
33. Kalejaiye O, Amyotte PR, Pegg M, Cashdollar KL. Effectiveness of dust dispersion in the 20-L Siwek chamber. *J Loss Prev Process Ind.* 2010; 23:46–59.
34. ASTM E1515. Standard test method for minimum explosible concentration of combustible dust. ASTM International; West Conshohocken, PA: 2007.
35. ASTM E2019. Standard test method for minimum ignition energy of a dust cloud in air. ASTM International; West Conshohocken, PA: 2013.
36. Randeberg E, Eckhoff RK. Measurement of minimum ignition energies of dust clouds in the < 1 mJ region. *J Hazardous Materials.* 2007; 140:237–244.
37. ASTM E1491. Standard test method for minimum autoignition temperature of dust clouds. ASTM International; West Conshohocken, PA: 2012.
38. Cornillault J. Particle Size Analyzer. *Applied Optics.* 1972; 11(2):265–268. [PubMed: 20111492]
39. Stephan, CR. US MSHA Report No 01-066-90. Pittsburgh, PA: 1990. *Coal Dust as a Fuel for Fires and Explosions.*
40. Woskoboienko F. Explosibility of Victoria brown coal dust. *Fuel.* 1988; 67:1062–1068.
41. Field, P. *Dust Explosions.* Elsevier; Amsterdam: 1982. cited in [8]
42. European Committee for Biological Effects of Carbon Black. *A Comparative Study of Soot and Carbon Black.* Cabot Corp; Boston, MA: Jan. 1984 Bulletin No. 2 cited in [8]
43. Cashdollar, KL.; Hertzberg, M.; Conti, RS. Explosion hazards of oil shale dusts: limits, pressures and ignitability. In: Gary, JH., editor. *Proceedings of the 17th Oil Shale Symposium.* Colorado School of Mines Press; Golden, CO: 1984. p. 243-254.

44. Holleman, AF.; Wiberg, E.; Wiberg, N. Inorganic Chemistry. Academic Press; San Diego: 2001. p. 810

Author Manuscript

Author Manuscript

Author Manuscript

Author Manuscript

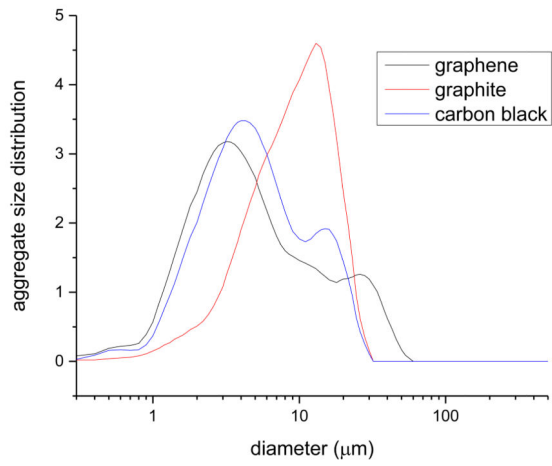
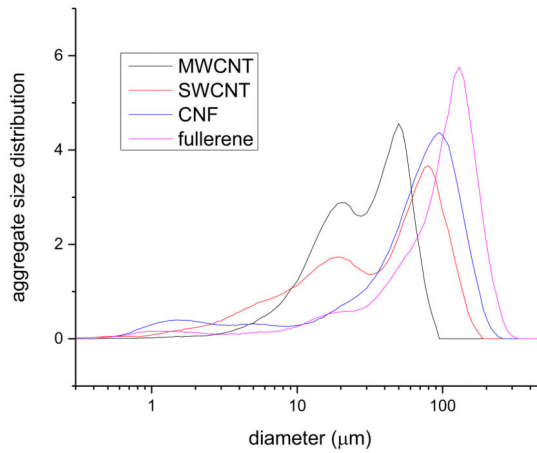
**Figure 1a****Figure 1b**

Figure 1. Aggregate particle size distributions as measured by light scattering: a) graphene, graphite, carbon black; b) MWCNT, SWCNT, carbon nanofibers (CNF), fullerene.

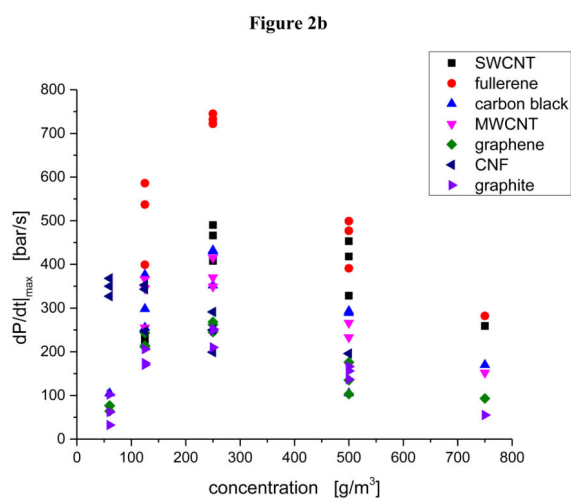
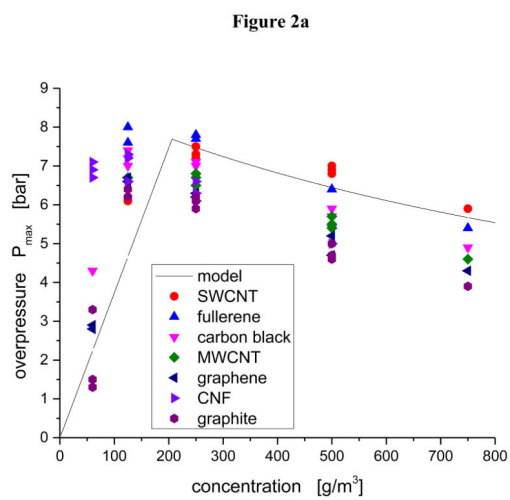


Figure 2. Concentration dependence of explosion parameters: a) maximum experimental overpressure, P_m , with thermodynamic curve (solid line) for graphite; b) maximum dP/dt .

Table 1

Explosion parameters of selected carbonaceous nanomaterials.

Material	P_{max} [bar]	$P_m(500)$ [bar]	K_{St} [bar·m/s]	$K(500)$ [bar·m/s]	MEC [g/m ³]	MIE [kJ]	MIT _{cloud} [°C]	$v = K_{St}/P_{max}$ [m/s]
fullerene	8.0	6.5	199	101	17	< 0.25	550	25
SWCNT	7.3	6.8	123	79	64	0.25 – 0.5	570	17
carbon black	7.2	5.9	112	61	53	0.25 – 0.5	> 600	16
MWCNT	6.7	5.9	104	57	48	0.25 – 0.5	> 600	16
graphene	6.6	5.5	70	46	73	0.5 – 1.0	> 600	11
CNF	7.1	5.4	96	15	51	1.0 – 2.5	> 600	14
graphite	6.3	4.6	64	27	92	1.0 – 2.5	> 600	10